

# Hydrogen bonding in enantiomeric *versus* racemic mono-carboxylic acids; a case study of 2-phenoxypropionic acid

Henning Osholm Sørensen and  
Sine Larsen\*

Centre for Crystallographic Studies, Department  
of Chemistry, University of Copenhagen,  
Universitetsparken 5, DK-2100 Copenhagen,  
Denmark

Correspondence e-mail: sine@ccs.ki.ku.dk

Received 23 September 2002

Accepted 22 November 2002

The structural and thermodynamic backgrounds for the crystallization behaviour of racemates have been investigated using 2-phenoxypropionic acid (PPA) as an example. The racemate of PPA behaves normally and forms a racemic compound that has a higher melting point and is denser than the enantiomer. Low-temperature crystal structures of the pure enantiomer, the enantiomer cocrystallized with *n*-alkanes and the racemic acid showed that hydrogen-bonded dimers that form over crystallographic symmetry elements exist in all but the structure of the pure enantiomer. A database search for optically pure chiral mono-carboxylic acids revealed that the hydrogen-bonded cyclic dimer is the most prevalent hydrogen-bond motif in chiral mono-carboxylic acids. The conformation of PPA depends on the hydrogen-bond motif; the antiplanar conformation relative to the ether group is associated with a catemer hydrogen-bonding motif, whereas the more abundant synplanar conformation is found in crystals that contain cyclic dimers. Other intermolecular interactions that involve the substituent of the carboxylic group were identified in the crystals that contain the cyclic dimer. This result shows how important the nature of the substituent is for the crystal packing. The differences in crystal packing have been related to differences in melting enthalpy and entropy between the racemic and enantiomeric acids. In a comparison with the equivalent 2-(4-chlorophenoxy)-propionic acids, the differences between the crystal structures of the chloro and the unsubstituted acid have been identified and related to thermodynamic data.

## 1. Introduction

The prediction of the crystal packing for simple organic compounds is one of today's scientific challenges. Despite significant activity in this field, there is no software available that can reliably predict the packing in simple molecular crystals (Beyer *et al.*, 2001; Gavezzotti, 2002; Motherwell *et al.*, 2002). The unambiguous assignment of the energetically most favourable crystal packing is difficult because molecular crystals can form different polymorphs with very similar energies and because all the facets of intermolecular interactions may not be sufficiently accounted for in the models employed to describe interatomic interactions in crystals.

Investigations of the crystal structures of an enantiomer and its corresponding racemic compound, which is composed of two enantiomers in equal amounts, offer, like polymorphs, a unique opportunity to investigate the interactions of the same molecule in different crystalline environments. Only interactions between molecules of the same chirality are possible in crystals of the enantiomer, whereas interactions between

molecules of the same and opposite chirality are possible in the racemic compound. The differences in melting entropy and enthalpy between the racemic compound and its enantiomer provide the thermodynamic background that, combined with an analysis of intermolecular interactions in the crystal, can give valuable insight into the determinants of crystal stability.

We decided that chiral mono-carboxylic acids with no other functional groups could be desirable targets for comparative studies of the crystal packing in enantiomeric and racemic crystals because the hydrogen-bond interactions between carboxylic groups have been so thoroughly investigated (Leiserowitz, 1976; Berkovitch-Yellin & Leiserowitz, 1982; Gavezzotti & Filippini, 1994). Two different hydrogen-bonding motifs are seen in these types of compounds: a cyclic dimer (Fig. 1c), and a catemer motif that links the carboxylic acids into infinite chains (Figs. 1a and 1b) either through the symmetry of a twofold screw axis or through glide planes. The cyclic dimer is the most abundant hydrogen-bond motif

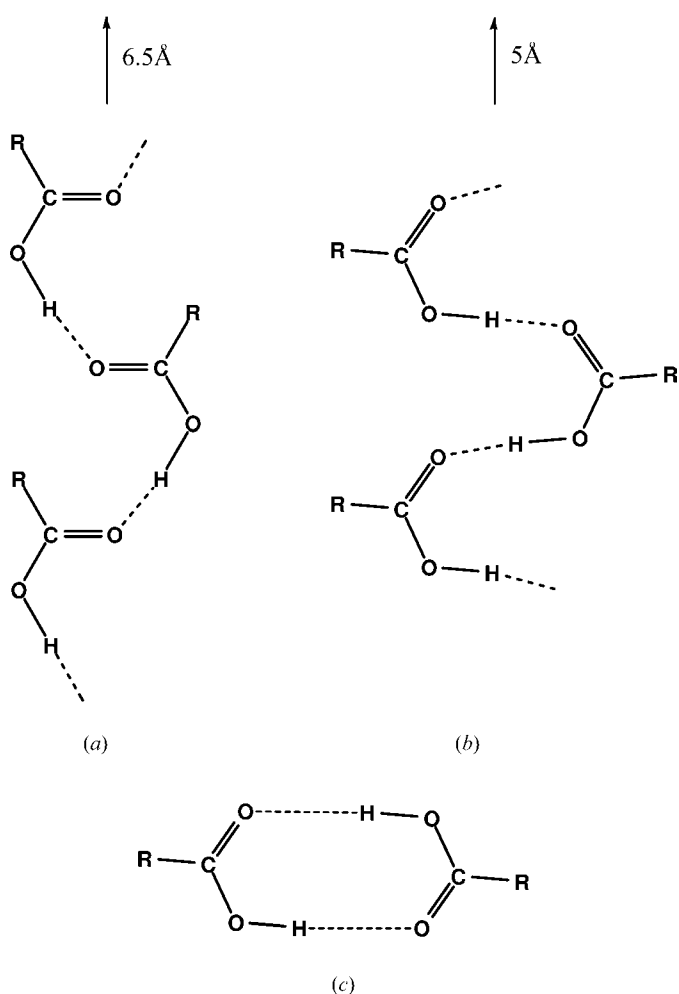


**Figure 1**  
The simple monofunctional carboxylic acids have only two possible motifs: the catemer motif shown in (a) and (b), which are the two limiting submotifs (variations that fall between these motifs are possible), and the dimer motif shown in (c). The number above the motifs is the approximate axis length in the chain direction of (a)–(b).

(Gavezzotti & Filippini, 1994; Steiner, 2001; Allen *et al.*, 1999), which could indicate that this dimer corresponds to the lowest energy. Early theoretical calculations that were carried out for formic acid ( $R = H$ ) at the STO-3G level showed, however, that the catemer motif with a corresponding translational period of 6.5 Å represents the hydrogen-bond arrangement with the lowest energy (Del Bene & Kochenour, 1976; Karpfen, 1984). Subsequent calculations on acetic acid, which also forms a catemer motif in the solid phase (Jones & Templeton, 1958; Nahrungbauer, 1970; Jönsson, 1971), at different basis set levels gave similar results and showed that the catemer motif is stabilized through additional C–H...O hydrogen bonds (Turi & Dannenberg, 1994; Borisenko *et al.*, 1995; Nakabayashi *et al.*, 1999; Rovira & Novoa, 2000, 2001).

Recently the lattice energies for the crystal structures of small mono-carboxylic acids were calculated based on an *ab initio* based multipole model of the interatomic and intermolecular potential (Beyer & Price, 2000). No intrinsic energy differences between the structures with the dimer and those with the catemer hydrogen-bond motif were revealed in this study, and the authors concluded that the crystal packing and steric interactions of the other functional groups play a major role in determining the energy of the crystal structures. Whether a dimer or a catemer motif is formed appears to depend on the nature of the substituent  $R$ . If one or more H atoms are present in the  $\alpha$  position, C–H...O hydrogen bonds can stabilize the catemer chains. In the cyclic dimer the substituent cannot be expected to exert the same effect on the hydrogen-bond energy, but can influence the packing of the dimers.

The chiral mono-carboxylic acid 2-phenoxypropionic acid (oPPA) appears well suited for a comparative study of its enantiomeric oPPA and racemic rPPA forms. The acid conforms to the 'normal' behaviour with respect to crystallization of racemates (Jacques *et al.*, 1981) and forms a racemic compound that melts  $\sim 30$  K higher than the pure enantiomer (Gabard & Collet, 1986). Kennard *et al.* (1982) have performed a structure determination of the racemic acid based on room-temperature diffraction data. This determination revealed that the crystals contain the acid as cyclic dimers that are formed over a crystallographic inversion centre; a similar arrangement is obviously not possible in the crystals of the enantiomeric pure chiral acid. To determine the crystal packing for the enantiomeric acid, we have conducted structure determinations at low temperature. In our attempts to prepare crystals of oPPA we obtained one of two different crystal forms depending on the solvent used for recrystallization. The pure enantiomer oPPA was precipitated from a mixture of cyclohexane and chloroform, whereas crystals that contained disordered solvent molecules were obtained from a mixture of methylene chloride and petroleum ether (abbreviated oPPA+a). The structure of the racemic acid was re-determined at low temperature in order to allow comparisons between structures of similar accuracy. Furthermore, by comparing the results from the unsubstituted acid with those obtained previously for 2-(4-chlorophenoxy)propionic acid (Kennard *et al.*, 1982; Raghunathan *et al.*, 1982; Sørensen *et al.*,

1999) we have also been able to examine how a *para*-chloro substitution affects the crystal packing and thermodynamic behaviour.

## 2. Experimental

### 2.1. Preparation and crystallization

*R*-(+)-2-Phenoxypropionic acid was prepared as described by Gabard & Collet (1986). *S*-(-)-Ethylactate (35.6 g, 0.30 mol) and *p*-toluenesulfonyl chloride (47.6 g, 0.25 mol) were dissolved in xylene (200 ml). Triethylamine (32.9 g, 0.33 mol) was added dropwise during a 10 min period. The temperature was kept at 303–308 K. After the reaction mixture had been stirred overnight, it was poured over 1 M HCl/ice. The phases were separated and the xylene phase was washed twice with water and dried over Na<sub>2</sub>SO<sub>4</sub>. The xylene was then evaporated. *S*-(-)-2-(*p*-Toluenesulfonate)ethylactate (53.53 g, 78.8%) was obtained after distillation in vacuo (422–424 K at 0.7 Torr).

*S*-(-)-2-(*p*-Toluenesulfonate)ethylactate (40.2 g, 0.147 mol), phenol (15.4 g, 0.163 mol) and K<sub>2</sub>CO<sub>3</sub> (24 g, 0.174 mol) were dissolved in 240 ml warm acetonitrile. The reaction mixture was refluxed for 4 h. The precipitate was filtered on a Büchner funnel and washed with ether. An oil was obtained after evaporation. The ester was purified by elution through an Al<sub>2</sub>O<sub>3</sub> column with methylene chloride:hexane (9:1). The eluent was removed by evaporation. The purified ester was dissolved in methanol (200 ml) and hydrolysed with aqueous NaOH (15 ml, 50%). The mixture was refluxed for 1 h. After evaporation of the methanol the residue was dissolved in water and extracted with ether. The aqueous solution was acidified with 4 M HCl and extracted with ether. The ether phase was dried over Na<sub>2</sub>SO<sub>4</sub> and evaporated to give 17.05 g of the acid (70% yield from the ester). At this stage the enantiomeric excess should be 75%, as a result of partial racemization (Gabard & Collet, 1986). The acid was optically purified through the formation of its propylamine salt. The acid (12.87 g, 0.077 mol) was dissolved in boiling ethylacetate (40 ml) and propylamine (4.5 g, 0.076 mol) was added. After precipitation of the salt, it was recrystallized in ethylacetate (30 ml). The salt was decomposed in 1 M aqueous HCl (100 ml) and extracted twice with ether. The ether phase was separated and dried over Na<sub>2</sub>SO<sub>4</sub> before evaporation, which resulted in an oil. A small amount of the oil was moved to a tube and cooled on ice. The crystals obtained were used to seed the oil.

The specific rotation (1.2 g ml<sup>-1</sup> ethanol) was determined to +34.4° [literature states +39.3° for the optically pure compound (Weast, 1972)]. The enantiomeric excess was calculated to be 87%, so further purification was necessary to obtain the optically pure compound. The acid was dissolved in warm ethylacetate and an equimolar amount of propylamine was added. The salt was recrystallized in ethylacetate three times before the salt was decomposed in 1 M HCl. The pure optically active *R*-(+)-2-phenoxypropionic acid was obtained upon extraction with ether and evaporation. Recrystallization

of the acid in cyclohexane:chloroform (1:9) led to the crystal form oPPA. Recrystallization of the acid in warm methylene chloride and petroleum ether 333–353 K gave another crystal form oPPA+a by incorporation of *n*-alkanes from the solvent. (±)-2-Phenoxypropionic acid (Aldrich) (0.103 g) was recrystallized in 20 ml hot water to give suitable crystals of the racemic acid rPPA.

### 2.2. X-ray crystallography

An Enraf–Nonius CAD-4 diffractometer with graphite monochromated Cu K $\alpha$  radiation ( $\lambda = 1.54184 \text{ \AA}$ ) was used for the data collections on single crystals cooled to 122.4 (5) K. Five standard reflections were measured every 166.7 min; these reflections showed no decay during the collections for the two optically active compounds but a decay of 5.8% for the racemic compound. Further details of the data collections are given in Table 1.<sup>1</sup>

The data reductions were performed with the program package DREAR (Blessing, 1987). The data were corrected for background, Lorentz, polarization and absorption effects (Detitta, 1985). The space group determinations were based on an analysis of the Laue class and the systematically absent reflections. The symmetry-related reflections were averaged according to the symmetry of the crystal classes.

The structures were solved by direct methods using SHELXS97 (Sheldrick, 1990) and refined by full matrix least-squares with SHELXL97 (Sheldrick, 1997) [minimizing  $\sum w(|F_o|^2 - |F_c|^2)^2$ ]. All reflections were used in the refinements. After refinement of the positional and anisotropic displacement parameters of all non-H atoms the positions of the H atoms could be located in the difference-Fourier maps. Positions and isotropic temperature factors of the H atoms were refined freely without constraints. In the difference-Fourier map of oPPA+a two peaks were located, which were modelled as two C atoms. The thermal parameters of these atoms were elongated along the *b* axis, because the C atoms are part of longer *n*-alkane(s) that were incorporated from the petroleum ether used as recrystallizing agent. It was not possible to establish the actual size of the hydrocarbons. The absolute structures were set to the known configuration and confirmed by the Flack parameter (Flack, 1983). The data of oPPA and rPPA were corrected for extinction. Details on the structure refinements are given in Table 1.

### 2.3. Computational details

Gaussian98 (Frisch *et al.*, 1998) was used for all *ab initio* calculations. The calculations were performed at the RHF/6-31G(*d,p*) and B3LYP/6-31G(*d,p*) levels as implemented in Gaussian98. Initial geometries were taken from the experimental structures of rPPA (synplanar conformation) and oPPA (antiplanar conformation). At each computational level two types of calculations were performed as follows: (i) the torsion angles C6–C1–O7–C8, C1–O7–C8–C9 and

<sup>1</sup>Supplementary data for this paper are available from the IUCr electronic archives (Reference: OS0103). Services for accessing these data are described at the back of the journal.

**Table 1**  
Experimental details.

	oPPA	oPPA+a	rPPA
<b>Crystal data</b>			
Chemical formula	C <sub>9</sub> H <sub>10</sub> O <sub>3</sub>	C <sub>9</sub> H <sub>10</sub> O <sub>3</sub> ·C <sub>x</sub> H <sub>2x</sub> (4 ≤ x ≤ 6)	C <sub>9</sub> H <sub>10</sub> O <sub>3</sub>
<i>M<sub>r</sub></i>	166.17	166.17 (224.29 to 252.35)	166.17
Cell setting, space group	Monoclinic, <i>P</i> 2 <sub>1</sub>	Orthorhombic, <i>P</i> 2 <sub>1</sub> 2 <sub>1</sub> 2	Monoclinic, <i>C</i> 2/ <i>c</i>
<i>a</i> , <i>b</i> , <i>c</i> (Å)	8.5312 (15), 4.8321 (8), 10.125 (2)	25.510 (3), 5.2248 (8), 7.6494 (9)	28.781 (3), 5.2554 (8), 10.9534 (15)
α, β, γ (°)	90.00, 92.031 (16), 90.00	90.00, 90.00, 90.00	90.00, 97.816 (10), 90.00
<i>V</i> (Å <sup>3</sup> )	417.14 (14)	1019.6 (2)	1641.4 (4)
<i>Z</i>	2	4	8
<i>D<sub>x</sub></i> (Mg m <sup>-3</sup> )	1.323	1.265	1.345
Radiation type	Cu <i>K</i> α	Cu <i>K</i> α	Cu <i>K</i> α
No. of reflections for cell parameters	20	20	25
θ range (°)	39.3–40.2	39.4–40.6	39.2–41.9
μ (mm <sup>-1</sup> )	0.83	0.75	0.84
Temperature (K)	122.4 (5)	122.4 (5)	122.4 (5)
Crystal form, colour	Plate, colourless	Plate, colourless	Needle, colourless
Crystal size (mm)	0.48 × 0.21 × 0.06	0.62 × 0.20 × 0.07	0.41 × 0.17 × 0.10
<b>Data collection</b>			
Diffractometer	Enraf–Nonius CAD-4	Enraf–Nonius CAD-4	Enraf–Nonius CAD-4
Data collection method	ω–2θ scan	ω–2θ scan	ω–2θ scan
Absorption correction	Numerical	Numerical	Numerical
<i>T<sub>min</sub></i>	0.770	0.787	0.805
<i>T<sub>max</sub></i>	0.954	0.951	0.925
No. of measured, independent and observed reflections	3609, 1714, 1697	5813, 2111, 2037	6057, 1697, 1624
Criterion for observed reflections	<i>I</i> > 2σ( <i>I</i> )	<i>I</i> > 2σ( <i>I</i> )	<i>I</i> > 2σ( <i>I</i> )
<i>R<sub>int</sub></i>	0.010	0.014	0.038
θ <sub>max</sub>	74.9	74.9	74.8
Range of <i>h</i> , <i>k</i> , <i>l</i>	–10 ⇒ <i>h</i> ⇒ 10 –6 ⇒ <i>k</i> ⇒ 6 –12 ⇒ <i>l</i> ⇒ 12	–31 ⇒ <i>h</i> ⇒ 31 –6 ⇒ <i>k</i> ⇒ 6 –9 ⇒ <i>l</i> ⇒ 9	–36 ⇒ <i>h</i> ⇒ 19 –6 ⇒ <i>k</i> ⇒ 6 –13 ⇒ <i>l</i> ⇒ 13
No. and frequency of standard reflections	5 every 166.7 min	5 every 166.7 min	5 every 166.7 min
Intensity decay (%)	None	None	5.8
<b>Refinement</b>			
Refinement on	<i>F</i> <sup>2</sup>	<i>F</i> <sup>2</sup>	<i>F</i> <sup>2</sup>
<i>R</i> [ <i>F</i> <sup>2</sup> > 2σ( <i>F</i> <sup>2</sup> )], <i>wR</i> ( <i>F</i> <sup>2</sup> ), <i>S</i>	0.022, 0.058, 1.05	0.040, 0.119, 1.13	0.032, 0.087, 1.03
No. of reflections	1714	2111	1697
No. of parameters	150	167	150
H-atom treatment	Refined independently	Refined independently	Refined independently
Weighting scheme	$w = 1/[\sigma^2(F_o^2) + (0.0357P)^2 + 0.0553P]$ where $P = (F_o^2 + 2F_c^2)/3$	$w = 1/[\sigma^2(F_o^2) + (0.0694P)^2 + 0.3045P]$ where $P = (F_o^2 + 2F_c^2)/3$	$w = 1/[\sigma^2(F_o^2) + (0.0417P)^2 + 1.2118P]$ where $P = (F_o^2 + 2F_c^2)/3$
(Δ/σ) <sub>max</sub>	<0.001	<0.001	<0.001
Δρ <sub>max</sub> , Δρ <sub>min</sub> (e Å <sup>-3</sup> )	0.15, –0.13	0.51, –0.37	0.33, –0.22
Extinction method	<i>SHELXL</i>	None	<i>SHELXL</i>
Extinction coefficient	0.043 (2)		0.0066 (4)
Absolute structure	Flack (1983)	Flack (1983)	
Flack parameter	–0.03 (13)	0.0 (3)	

Computer programs: *Enraf–Nonius Express* (Enraf–Nonius, 1994); *DREADD* (Blessing, 1987); *DREAR* (Blessing, 1987); *SHELXS97* (Sheldrick, 1990); *SHELXL97* (Sheldrick, 1997); *ORTEPII* (Johnson, 1976).

O7–C8–C9–O10 were constrained to the values in the crystal structures and (ii) full geometry optimization was used.

### 3. Results and discussion

#### 3.1. Comparison of 2-phenoxypropionic acid in the different crystalline environments

The molecular structures of 2-phenoxypropionic acid (PPA) as observed in the racemic acid (rPPA) and in the two crystal structures that contain the enantiomeric form (oPPA and oPPA+a) are illustrated in Fig. 2. With the phenyl and the carboxylic acid groups conforming to planarity the confor-

mation of PPA can be described by the three torsion angles listed in Table 2. All three structures display almost coplanarity of the phenyl group and the ether group. It is obvious from Fig. 2 and Table 2 that the acid adopts similar conformations in rPPA and oPPA+a. In these two structures the C=O moiety of the carboxylic acid group adopts a synplanar conformation relative to the ether group. In contrast the carboxylic acid group in oPPA is in an antiplanar conformation. The deviation from the idealized synplanar conformation is most pronounced in rPPA, as illustrated by the value of the torsion angle O7–C8–C9–O10 [23.77 (13)°]. Note that these small conformational variations of PPA in the different crystalline environments do not lead to any variations in the

bond lengths and angles, which are virtually identical in rPPA and oPPA+a. Compared with the geometry of the antiplanar conformation observed in oPPA, in rPPA the carboxylic acid group is more tilted with respect to the C8—C9 bond, as reflected in the O10—C9—C8 and O11—C9—C8 angles. The averages of the angles in the PPA molecules with synplanar conformation are 123.7 (3)° and 111.8 (3)°, while the values

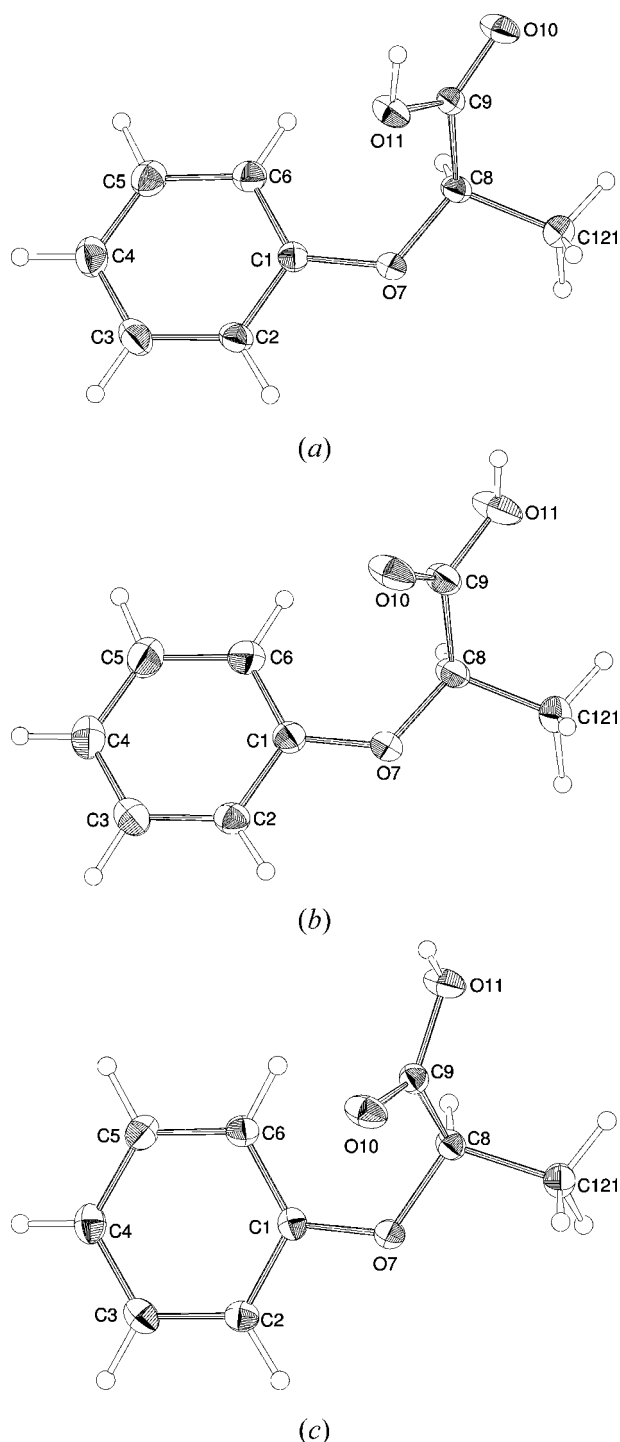


**Figure 2**  
ORTEP drawings of phenoxypropionic acid showing the labelling in the three different crystal forms: (a) optically active pure form, (b) optically active with incorporated solvent and (c) racemic form.

**Table 2**  
Selected bond lengths (Å), angles (°) and torsion angles (°).

	oPPA	oPPA+a	rPPA
<b>Bond lengths</b>			
O7—C1	1.3753 (12)	1.376 (2)	1.3729 (12)
O7—C8	1.4221 (12)	1.4226 (18)	1.4236 (12)
O10—C9	1.2169 (12)	1.214 (2)	1.2183 (13)
O11—C9	1.3086 (12)	1.307 (2)	1.3138 (13)
C1—C6	1.3913 (14)	1.388 (2)	1.3919 (15)
C1—C2	1.3963 (14)	1.391 (2)	1.3956 (14)
C2—C3	1.3867 (15)	1.390 (2)	1.3849 (15)
C3—C4	1.3922 (17)	1.384 (3)	1.3931 (16)
C4—C5	1.3817 (16)	1.383 (3)	1.3844 (16)
C5—C6	1.3925 (15)	1.397 (3)	1.3954 (15)
C121—C8	1.5192 (13)	1.521 (2)	1.5212 (14)
C8—C9	1.5242 (13)	1.525 (2)	1.5217 (14)
<b>Bond angles</b>			
C1—O7—C8	118.93 (7)	119.29 (13)	118.51 (8)
O7—C1—C6	125.29 (9)	124.95 (15)	124.96 (9)
O7—C1—C2	114.50 (8)	114.63 (14)	114.86 (9)
O7—C8—C121	106.77 (8)	106.21 (13)	106.39 (8)
O7—C8—C9	112.70 (8)	111.38 (12)	111.39 (8)
O10—C9—O11	124.81 (9)	124.49 (15)	124.50 (9)
O10—C9—C8	120.18 (9)	123.86 (14)	123.45 (9)
O11—C9—C8	114.99 (8)	111.64 (13)	111.99 (9)
<b>Torsion angles</b>			
C8—O7—C1—C6	−1.27 (14)	−6.10 (2)	−7.26 (14)
C1—O7—C8—C9	77.20 (10)	75.09 (18)	71.94 (11)
O7—C8—C9—O10	−178.23 (8)	7.00 (3)	23.77 (13)

observed in the antiplanar oPPA are 120.18 (9)° and 114.99 (8)°. In order to examine whether the opening of the O10—C9—O8 angle is correlated with the conformation of the O10—C9—C8—O7 moiety, the Cambridge Structural Database (CSD, version 5.22, October 2001; Allen & Kennard, 1993) was searched for organic structures that have *R* values below 10% and that contain the fragment C—O—C—COOH. The angles equivalent to C8—C9—O10 and C8—C9—O11 were compared for the two different conformations. In compounds with the synplanar conformation the averages of these angles are 123.7 (3)° and 111.7 (3)°, while the averaged values for the equivalent bond angles in molecules that display an antiplanar conformation are 119.2 (4)° and 115.5 (3)°. Scatter plots of the C8—C9—O10 angle against the torsion angle confirm the opening of the C8—C9—O10 angle for molecules in the synplanar conformation (Fig. 3). Thus the opening of the C8—C9—O10 angle seen in the rPPA structure is not a unique feature of this structure. This behaviour moves O10 further away from O7, which can be rationalized in terms of the larger negative charge of O10. The synplanar conformation is the more prevalent with an occurrence of 72%. Nevertheless our *ab initio* calculations conducted at the RHF and DFT/B3LYP level show an almost negligible energy difference between the two experimental conformations (0.3–0.6 kJ mol<sup>−1</sup>, Table 3) with the synplanar conformation having the lower energy. This picture is reversed for the full geometry-optimized structures. It is evident from Table 4 that rPPA has a geometry very close to the optimized structure, whereas the geometry of the antiplanar structure differs significantly from the experimental structure.

**Table 3**

Relative electronic energies ( $\text{kJ mol}^{-1}$ ) of PPA in the experimental conformations and in the most stable synplanar and antiplanar conformations calculated at the RHF and B3LYP levels with the 6-31G(*d,p*) basis set.

	oPPA	rPPA	$E(\text{oPPA}) - E(\text{rPPA})$
RHF level			
Experimental conformation	0.0	-0.3	+0.3
Optimized conformation	-3.6	-1.2	-2.4
B3LYP level			
Experimental conformation	0.0	-0.6	+0.6
Optimized conformation	-2.4	-1.2	-1.2

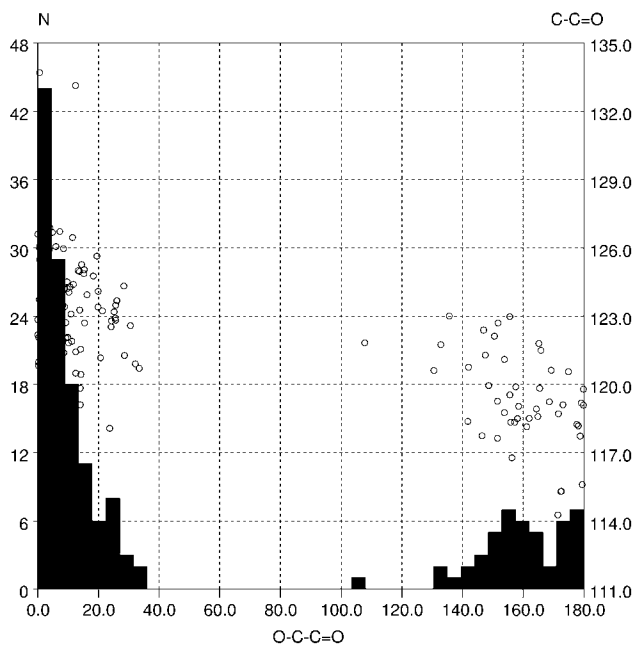
**Table 4**

Comparison of the torsion angles ( $^\circ$ ) from the geometry-optimized calculation at the B3LYP/6-31G(*d,p*) level with the experimental values.

	oPPA		rPPA	
	Exp	Opt	Exp	Opt
O7–C8–C9–O10	-178.2	-148.3	23.8	25.4
C1–O7–C8–C9	77.2	70.7	71.9	72.8
C8–O7–C1–C6	-1.3	-2.4	-7.3	-1.1

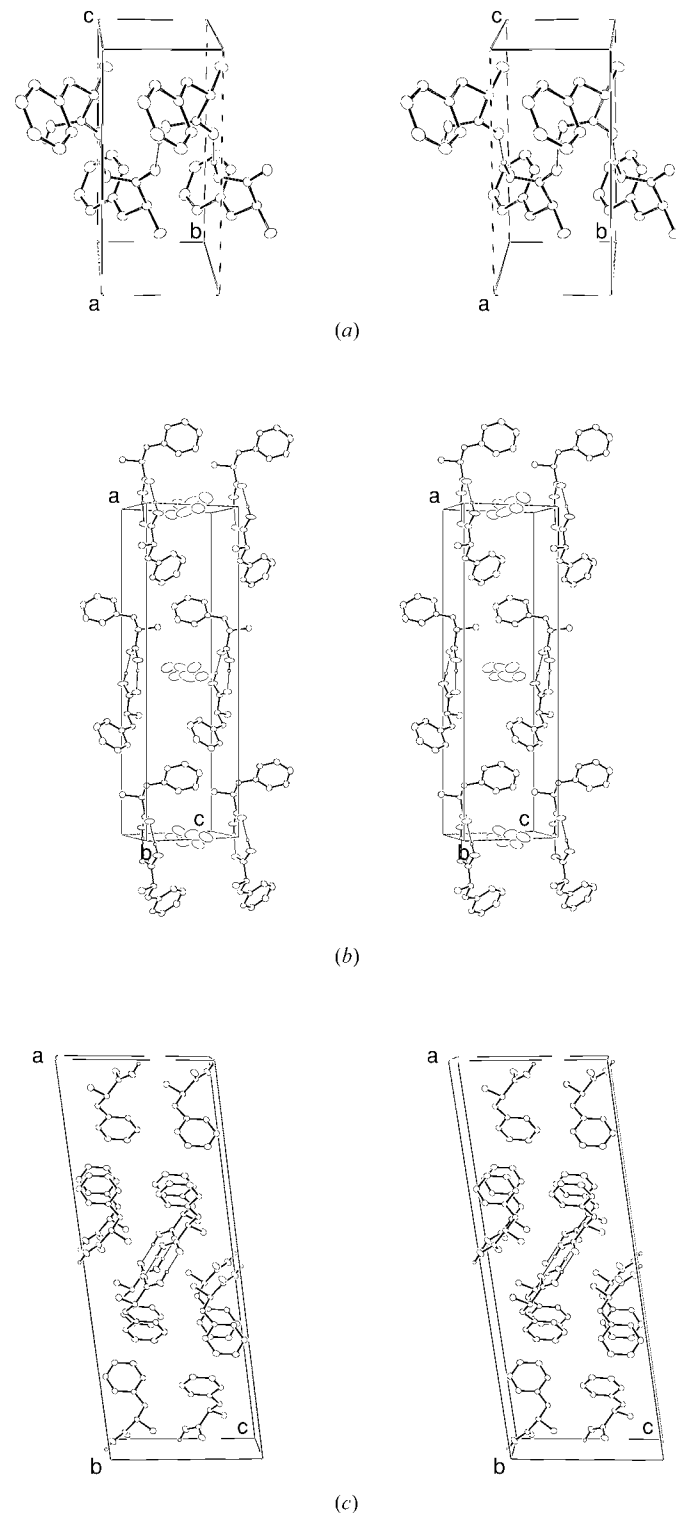
### 3.2. Intermolecular interactions

The difference between the molecular structure of PPA in the racemic and enantiomeric crystals originates in the differences in their intermolecular interactions. These interactions are illustrated by the packing diagrams in Fig. 4. The hydrogen bonds that connect the PPA molecules in the three structures are tabulated in Table 5. The twofold screw axis connects antiplanar PPA molecules into a catemer motif in oPPA. Cyclic carboxylic acid dimers connect the synplanar


**Figure 3**

The distribution of the torsion angles O–C–C=O extracted from the CSD is shown in the histogram. The open circles show the C–C=O angle as a function of the O–C–C=O torsion angle.

molecules in rPPA and oPPA+a. In both compounds the dimers are formed over crystallographic symmetry elements: an inversion centre in rPPA and a twofold axis in oPPA+a. The hydrogen-bond parameters appear identical in the three structures, with O10...O11 donor–acceptor distances of


**Figure 4**

Stereo drawings showing the crystal packing in the three different crystal forms: (a) optically active pure form, (b) optically active with incorporated solvent and (c) racemic form.

**Table 5**  
Hydrogen bond lengths (Å) and angles (°) in oPPA+a, oPPA and rPPA.

	oPPA	oPPA+a	rPPA
O11—H11···O10			
<i>D</i> ··· <i>A</i>	2.6677 (11)	2.6685 (18)	2.6584 (11)
H··· <i>A</i>	1.74 (2)	1.78 (3)	1.74 (2)
< <i>D</i> —H··· <i>A</i>	170 (2)	178 (3)	178 (2)
Symmetry	(1 - <i>x</i> , <i>y</i> - ½, 1 - <i>z</i> )	(2 - <i>x</i> , 2 - <i>y</i> , <i>z</i> )	(1 - <i>x</i> , - <i>y</i> , 1 - <i>z</i> )
C121—H123···O10			
<i>D</i> ··· <i>A</i>		3.462 (2)	3.450 (2)
H··· <i>A</i>		2.53 (3)	2.52 (2)
< <i>D</i> —H··· <i>A</i>		150 (2)	155 (1)
Symmetry		( <i>x</i> , 1 + <i>y</i> , <i>z</i> )	( <i>x</i> , 1 + <i>y</i> , <i>z</i> )

2.66 Å and hydrogen-acceptor distances of around 1.75 Å for the perfect two-centre hydrogen bonds. The translational period of the twofold screw axis involved in creating the catemer hydrogen-bond motif found in oPPA is 4.8 Å. This short period leads to a catemer with almost parallel hydrogen bonds so that O10 and O11 are 0.13 Å closer [O10···O11 = 2.9070 (13) Å] than the sum of the van der Waals radii. This motif has previously been argued to be the energetically least favourable among the motifs that link the carboxylic acid groups (Berkovitch-Yellin & Leiserowitz, 1982). There are weaker C—H···O hydrogen bonds in both rPPA and oPPA+a between the methyl group and an O10 atom from a molecule related to the methyl group by translational symmetry along the *b* axis, which has a translational period around 5.25 Å. Furthermore, rPPA possesses an additional hydrogen C—H···O hydrogen bond to the ether O atom.

Interactions between the phenyl groups are another common feature of the packing in the three different compounds. It is apparent from Fig. 4 that the phenyl groups exhibit a herringbone arrangement (*C<sub>ar</sub>*—H···*C<sub>ar</sub>*) with very similar interplanar angles in rPPA [89.42 (3)°], oPPA [89.77 (3)°] and oPPA+a [88.67 (5)°]. The crystal structure of the latter compound must also be influenced by the interactions between PPA and the enclosed solvent, but because of the pronounced disorder of the solvent molecules it is not possible to assign any specific interactions.

### 3.3. Influence of the solvent on the crystal packing

Inspection of the packing diagram of oPPA+a in Fig. 4 illustrates why this arrangement of PPA molecules is not possible for the crystallization of PPA without a solvent. The hydrogen-bond arrangement of the cyclic dimers and interacting phenyl groups creates tunnels parallel to the *b* axis with a cross section 6.0 × 7.7 Å. The *n*-alkanes from the solvent fill this tunnel and can thereby stabilize the crystal packing by interactions with the phenyl groups. The tunnels are large enough to accommodate *n*-alkanes but not the larger molecules of cyclohexane and chloroform that were present in the crystallization conditions that resulted in unsolvated oPPA. rPPA and oPPA have comparable crystal densities with rPPA being the more dense. Both are significantly denser than

**Table 6**  
The distribution in the CSD (version 5.22, October 2001) of hydrogen-bond types in chiral mono-carboxylic acids crystallized in enantiomorphous space groups.

The two structures oPPA and oPPA+a have been included.

Hydrogen-bond type	Space group	Number	% of all acids
Catemers	<i>P</i> <sub>2</sub> <sub>1</sub> <i>2</i> <sub>1</sub> <i>2</i> <sub>1</sub>	4	24.4
	<i>P</i> <sub>2</sub> <sub>1</sub>	7	
	Total	11	
Asymmetric dimer	<i>P</i> <sub>1</sub>	2	60.0
	<i>P</i> <sub>2</sub> <sub>1</sub>	16	
	<i>P</i> <sub>2</sub> <sub>1</sub> <i>2</i> <sub>1</sub> <i>2</i> <sub>1</sub>	8	
	<i>P</i> <sub>3</sub> <sub>1</sub>	1	
	Total	27	
Symmetric dimer	<i>P</i> <sub>2</sub> <sub>1</sub> <i>2</i> <sub>1</sub> <i>2</i>	2	6.7
	<i>C</i> <sub>2</sub>	1	
	Total	3	
OH···O <sub>ether</sub>	<i>P</i> <sub>2</sub> <sub>1</sub> <i>2</i> <sub>1</sub> <i>2</i> <sub>1</sub>	1	2.5
	<i>P</i> <sub>2</sub> <sub>1</sub>	3	
	Total	4	

oPPA+a, even if it has the tunnel completely filled with *n*-alkanes (*D<sub>x</sub>* = 1.265 g cm<sup>-3</sup>, Table 1). Without alkanes in the tunnel the density is 1.083 g cm<sup>-3</sup>.

### 3.4. Hydrogen-bond patterns in chiral mono-carboxylic acids

The tendency of mono-carboxylic acids to form either cyclic dimers or catemers has been investigated previously, first by Gavezzotti & Filippini (1994) and later by Allen *et al.* (1999) using the CSD (Allen & Kennard, 1993). These investigations, which did not distinguish between chiral and achiral compounds [the results of Allen *et al.* (1999) are shown in brackets if they differ from the results of Gavezzotti & Filippini (1994)], revealed that more than 95% of the mono-functional carboxylic acids form cyclic dimers and only 5% form the catemer motif. Of the 95% that form cyclic dimers, 73% (75%) are connected over an inversion centre. Because optically pure chiral compounds cannot crystallize over an inversion centre, the same distribution is not possible in the chiral acids. To examine the distribution of hydrogen-bond patterns in the optically pure chiral mono-carboxylic acids *R*-COOH, a search was conducted in the CSD (version 5.22, October 2001; Allen & Kennard, 1993). In order to obtain a reasonable number of structures we allowed them to contain halogens, silicon and (thio)ether groups, which do not display a high hydrogen-bond acceptor ability. Only structures with *R* values of less than 10% were retrieved. The hydrogen-bond patterns in the 43 structures that resulted from this search were analysed with the program *Cerius*<sup>2</sup> (MSI, 1997). Table 6 shows the distribution of hydrogen-bond types observed in these structures and in those of oPPA and oPPA+a. Four of the structures form neither catemers nor dimers but instead form hydrogen bonds to an ether O atom. Though the structures cannot form dimers over an inversion centre, the carboxylic acid dimer is still the prevalent hydrogen-bond motif in more than half of the acids (67%). 60% of the

carboxylic acid dimers are asymmetric and are formed in structures with at least two molecules in the asymmetric unit. The catemer motif is more abundant in the chiral monocarboxylic acids: 24% compared to 5% in general (Allen *et al.*, 1999; Gavezzotti & Filippini, 1994). Of the 11 structures that form catemer motifs, only HEKWOJ (Jong & Chen, 1994) and FIXQEI (Sørensen *et al.*, 1999) adopt the energetically most favourable motif shown in Fig. 1(a). Considering that HEKWOJ is the molecule with the second largest substituent ( $R = C_{29}H_{47}$ ) it is noteworthy that this compound forms the catemer motif that is usually found in acids with small substituents (Leiserowitz, 1976).

The abundance of cyclic carboxylic dimers should not lead to the assumption that this is the energetically most favourable hydrogen-bonding motif, since the crystal packing in all the compounds examined is influenced by other intermolecular interactions. This fact emphasizes how important it is to take the nature of the substituent into account in the prediction of crystal structures.

### 3.5. Influence of a chloro substitution

The racemic compounds of both the 2-(4-chlorophenoxy)propionic acid (rCIPPA) and the unsubstituted rPPA crystallize in the same space group and form symmetric hydrogen-bonded dimers over the crystallographic inversion centre. Likewise, in both compounds the packing along the *c* axis comprises alternating layers of carboxylic acid and phenyl groups. Weak C—H...O hydrogen bonds are present in both structures:<sup>2</sup> rCIPPA has a slightly shorter H121...O10 distance (2.57 Å) and a longer H5...O7 distance (2.88 Å). The only prominent difference between the two structures is the presence in rCIPPA of C—H...Cl hydrogen bonds formed over another inversion centre, which result in a difference in the interactions between the phenyl groups. The  $C_{ar}$ —H... $C_{ar}$  interactions that are present in rPPA in addition to the phenyl–phenyl stacking are not observed in rCIPPA. The chloro substitution also creates significant differences between the packing in the enantiomeric compounds of PPA. Both contain hydrogen-bonded catemers along the twofold screw axis, but oPPA adopts the energetically least favourable motif (Fig. 1b) and *R*-(+)-2-(4-chlorophenoxy)propionic acid (oCIPPA) the most favourable (Fig. 1a). The catemer motif in oCIPPA is stabilized by a C—H...O hydrogen bond between H81 and O10 [H81...O10, 2.639 (18) Å], thus forming a pseudo dimer as observed in acetic acid (Jones & Templeton, 1958; Nahrungbauer, 1970; Jönsson, 1971). oCIPPA, like the racemic compound rCIPPA, contains only phenyl–phenyl stacking.

### 3.6. Relation to the thermodynamic properties

The similarities and differences in the crystal packings of the racemic and enantiomeric unsubstituted and chloro-substituted 2-phenoxypropionic acids should be reflected in the variations of the thermodynamic properties summarized in

<sup>2</sup> The H...O distance cutoff has been chosen according to Steiner (1996).

**Table 7**

Thermodynamic data taken from Gabard & Collet (1986).

$\Delta G^\ominus$  has been calculated using equation (1).

	$T^f$ (K)		$\Delta H^f$ (kJ mol <sup>-1</sup> )		$\Delta S^f$ (J mol <sup>-1</sup> K <sup>-1</sup> )		$\Delta G^\ominus (T_{OA}^f)$ (kJ mol <sup>-1</sup> )
	Rac	OA	Rac	OA	Rac	OA	
PPA	388	359	33.1	22.6	85.2	63.0	-4.6
CIPPA	386	376	37.7	23.4	97.6	62.4	-3.2

Table 7. The melting points depend both on the enthalpy and on the entropy associated with the melting process ( $\Delta H^f = T^f \Delta S^f$ ). The melting enthalpy reflects the difference in energy for the molecule in the crystal and in the melt, and the entropy indicates the difference in 'ordering' between the two states. Table 7 reveals a pronounced difference between the racemic and enantiomeric acids in the thermodynamic properties associated with the melting process. The racemic acids have a heat of fusion more than 10 kJ mol<sup>-1</sup> higher and an entropy of fusion more than 22 J mol<sup>-1</sup> K<sup>-1</sup> higher than those of the enantiomeric acids. Assuming that the melts of oPPA and rPPA behave ideally the entropy of the racemic melt should be 5.8 J mol<sup>-1</sup> K<sup>-1</sup> higher than for the pure enantiomer because of the mixing entropy  $R \ln 2$  (Jacques *et al.*, 1994). However this can only account for a fraction of the observed difference.

The presence of the synplanar conformation in the racemic acids cannot be a consequence of the cyclic dimer alone, which would only require shifts of protons in the hydrogen-bond pattern, but rather of the additional C—H...O hydrogen-bond interactions that are formed in the racemic acid. The chloro-substituted acids have higher melting enthalpies than the unsubstituted acids. The difference amounts to 4.6 kJ mol<sup>-1</sup> for the racemic acids. rPPA and rCIPPA have similar intermolecular interactions, but rCIPPA possesses additional H...Cl hydrogen bonds over an inversion centre, which can explain the higher melting enthalpy for rCIPPA. Furthermore these interactions fix the molecules in the crystal structure, thereby reducing their mobility, which could account for the larger entropy of fusion. Similar strong H...Cl interactions are not prevalent in oCIPPA, which forms the energetically most favourable catemer motif. The presence of the energetically less favoured catemer motif in oPPA could explain why it has a lower enthalpy of fusion. Note, however, that the energy difference is smaller than the 4 kJ mol<sup>-1</sup> calculated for the equivalent hydrogen patterns in formic acid. The enthalpy and entropy differences between the racemic and enantiomeric acids can be used to calculate  $\Delta G^\ominus$  for the reaction  $R + S \rightarrow RS$  (Gabard & Collet, 1986; Larsen & Marthi, 1997a),

$$\Delta G^\ominus(T) = \Delta H_{OA}^f(T_{OA}^f) - \Delta H_{rac}^f(T_{rac}^f) - T[\Delta S_{OA}^f(T_{OA}^f) - \Delta S_{rac}^f(T_{rac}^f) + R \ln 2], \quad (1)$$

where the  $R \ln 2$  term originates from the mixing entropy. This reaction is thermodynamically favoured for both PPA and CIPPA.



Our earlier studies of racemic and enantiomeric compounds dealt with systems that did not conform to the normal crystallization behaviour of racemates, e.g. the racemic compound melted at a lower temperature than the pure enantiomer. In these systems comprised of different halogen-substituted mandelic and 3-hydroxy-3-phenylpropionic acids all possible modes of hydrogen-bond interactions between hydroxy and carboxylic acid groups were encountered (Larsen & Marthi, 1994, 1995, 1997a,b). These studies showed only small differences between hydrogen-bond interactions in the racemic and enantiomeric compounds. In contrast the 2-phenoxypropionic acids investigated here display pronounced differences in their hydrogen-bond interactions.

## 4. Conclusions

The observation that the racemic compounds of 2-phenoxypropionic acid and 2-(4-chlorophenoxy)propionic acid have a higher melting enthalpy than the enantiomers can be related to differences in the hydrogen-bond interactions. However, analyses of the crystal structures for racemic and enantiomeric acids have revealed that the crystal packing also depends on a variety of intermolecular interactions. A complex interplay of these interactions may affect the conformational energy of the entities in the crystal. This study showed the importance of taking the nature of the substituent into account, when energy differences between the cyclic dimer and the catemer hydrogen-bond motif are discussed. It was also demonstrated that the crystal entropy may play a role in forming the most stable crystal form. The complexity encountered in the present systems of the determinants for thermodynamically stable crystal structure illustrate why it is still so difficult to perform crystal structure predictions by computational methods.

We thank Mr Flemming Hansen for help with the crystallographic experiments. The work is supported by grants from the Danish Natural Science Research Council and the Faculty of Science, University of Copenhagen.

## References

- Allen, F. H. & Kennard, O. (1993). *Chem. Des. Autom. News*, **8**, 31–37.
- Allen, F. H., Motherwell, W. D. S., Raithby, P. R., Shields, G. P. & Taylor, R. (1999). *New J. Chem.* **23**, 25–34.
- Berkovitch-Yellin, Z. & Leiserowitz, L. (1982). *J. Am. Chem. Soc.* **104**, 4052–4064.
- Beyer, T., Lewis, T. & Price, S. L. (2001). *Cryst. Eng. Commun.* **44**, 1–35.
- Beyer, T. & Price, S. L. (2000). *J. Phys. Chem.* **B104**, 2647–2655.
- Blessing, R. H. (1987). *Cryst. Rev.* **1**, 3–58.
- Borisenko, K. B., Bock, C. W. & Hargittai, I. (1995). *J. Mol. Struct.* **332**, 161–169.
- Del Bene, J. E. & Kochenour, W. L. (1976). *J. Am. Chem. Soc.* **98**, 2041–2046.
- DeTitta, G. T. (1985). *J. Appl. Cryst.* **18**, 75–79.
- Enraf–Nonius (1994). *Enraf–Nonius Express*. Enraf–Nonius, Delft, The Netherlands.
- Flack, H. D. (1983). *Acta Cryst.* **A39**, 876–881.
- Frisch, M. J., Trucks, G. W., Schlegel, H. B., Scuseria, G. E., Robb, M. A., Cheeseman, J. R., Zakrzewski, V. G., Montgomery, J. A. Jr, Stratmann, R. E., Burant, J. C., Dapprich, S., Millam, J. M., Daniels, A. D., Kudin, K. N., Strain, M. C., Farkas, O., Tomasi, J., Barone, V., Cossi, M., Cammi, R., Mennucci, B., Pomelli, C., Adamo, C., Clifford, S., Ochterski, J., Petersson, G. A., Ayala, P. Y., Cui, Q., Morokuma, K., Malick, D. K., Rabuck, A. D., Raghavachari, K., Foresman, J. B., Cioslowski, J., Ortiz, J. V., Baboul, A. G., Stefanov, B. B., Liu, G., Liashenko, A., Piskorz, P., Komaromi, I., Gomperts, R., Martin, R. L., Fox, D. J., Keith, T., Al-Laham, M. A., Peng, C. Y., Nanayakkara, A., Gonzalez, C., Challacombe, M., Gill, P. M. W., Johnson, B., Chen, W. W., Wong, M., Andres, J. L., Gonzalez, C., Head-Gordon, M., Replogle, E. S. & Pople, J. A. (1998). *Gaussian98*. Revision A.7. Gaussian, Inc., Pittsburgh, PA, USA.
- Gabard, J. & Collet, A. (1986). *Nouveau J. Chim.* **10**, 685–690.
- Gavezzotti, A. (2002). *Synlett*, **2**, 201–214.
- Gavezzotti, A. & Filippini, G. (1994). *J. Phys. Chem.* **98**, 4831–4837.
- Jacques, J., Collet, A. & Wilen, S. H. (1994). *Enantiomers, Racemates and Resolutions*. Florida: Krieger.
- Jacques, J., Leclercq, M. & Brienne, M. J. (1981). *Tetrahedron*, **37**, 1727–1733.
- Johnson, C. K. (1976). *ORTEPII*. Report ORNL-5138. Oak Ridge National Laboratory, Tennessee, USA.
- Jones, R. E. & Templeton, D. H. (1958). *Acta Cryst.* **11**, 484–487.
- Jong, T.-T. & Chen, C.-T. (1994). *Acta Cryst.* **C50**, 1326–1328.
- Jönsson, P.-G. (1971). *Acta Cryst.* **B27**, 893–898.
- Karpfen, A. (1984). *Chem. Phys.* **88**, 415–423.
- Kennard, C. H. L., Smith, G. & White, A. H. (1982). *Acta Cryst.* **B38**, 868–875.
- Larsen, S. & Marthi, K. (1994). *Acta Cryst.* **B50**, 373–381.
- Larsen, S. & Marthi, K. (1995). *Acta Cryst.* **B51**, 338–346.
- Larsen, S. & Marthi, K. (1997a). *Acta Cryst.* **B53**, 803–811.
- Larsen, S. & Marthi, K. (1997b). *Acta Cryst.* **B53**, 280–292.
- Leiserowitz, L. (1976). *Acta Cryst.* **B32**, 775–802.
- Motherwell, W. D. S., Ammon, H. L., Dunitz, J. D., Dzyabchenko, A., Erk, P., Gavezzotti, A., Hofmann, D. W. M., Leusen, F. J. J., Lommerse, J. P. M., Mooij, W. T. M., Price, S. L., Scheraga, H., Schweizer, B., Schmidt, M. U., van Eijck, B. P., Verwer, P. & Williams, D. E. (2002). *Acta Cryst.* **B58**, 647–661.
- MSI (1997). *Cerius<sup>2</sup> User Guide*. Molecular Simulations Inc., San Diego, USA.
- Nahringbauer, I. (1970). *Acta Chem. Scand.* **24**, 453–462.
- Nakabayashi, T., Kosugi, K. & Nishi, N. (1999). *J. Phys. Chem.* **A103**, 8595–8603.
- Raghunathan, S., Chandrasekhar, K. & Pattabhi, V. (1982). *Acta Cryst.* **B38**, 2536–2538.
- Rovira, C. & Novoa, J. J. (2000). *J. Chem. Phys.* **113**, 9208–9216.
- Rovira, C. & Novoa, J. J. (2001). *J. Phys. Chem.* **B105**, 1710–1719.
- Sheldrick, G. M. (1990). *Acta Cryst.* **A46**, 467–473.
- Sheldrick, G. M. (1997). *SHELXL97. Program for the Refinement of Crystal Structures*. University of Göttingen, Germany.
- Sørensen, H. O., Collet, A. & Larsen, S. (1999). *Acta Cryst.* **C55**, 953–956.
- Steiner, T. (1996). *Cryst. Rev.* **6**, 1–57.
- Steiner, T. (2001). *Acta Cryst.* **B57**, 103–106.
- Turi, L. & Dannenberg, J. J. (1994). *J. Am. Chem. Soc.* **116**, 8714–8721.
- Weast, R. C. (1972). *Handbook in Chemistry and Physics*, 53rd ed. Cleveland, OH: The Chemical Rubber Co.